High-affinity monoclonal IgA regulates gut microbiota and prevents colitis in mice

Shinsaku Okai, Fumihito Usui, Shuhei Yokota, Yusaku Hori-i, Makoto Hasegawa, Toshinobu Nakamura, Manabu Kurosawa, Seiji Okada, Kazuya Yamamoto, Eri Nishiyama, Hiroshi Mori, Takuji Yamada, Ken Kurokawa, Satoshi Matsumoto, Masanobu Nanno, Tomoaki Naito, Yohei Watanabe, Tamotsu Kato, Eiji Miyauchi, Hiroshi Ohno, Reiko Shinkura

This file includes:

Present address of Shinsaku Okai, Fumihito Usui and Reiko Shinkura:
Applied Immunology, Graduate School of Biological Sciences,
Nara Institute of Science and Technology
Ikoma, Nara 630-0192, Japan

High-affinity monoclonal IgA regulates gut microbiota and prevents colitis in mice

Shinsaku Okai, [1, 13] Fumihito Usui, [1, 13] Shuhei Yokota, [1] Yusaku Hori-i, [1] Makoto Hasegawa, [2] Toshinobu Nakamura, [3] Manabu Kurosawa, [4] Seiji Okada, [5] Kazuya Yamamoto, [6] Eri Nishiyama, [6] Hiroshi Mori, [6] Takuji Yamada, [6] Ken Kurokawa, [7] Satoshi Matsumoto, [8] Masanobu Nanno, [8] Tomoaki Naito, [8] Yohei Watanabe, [8] Tamotsu Kato, [9] Eiji Miyauchi, [9] Hiroshi Ohno, [9, 10, 11] Reiko Shinkura[1, 12*]

[1]Department of Immunology, [2]Department of Protein Function Analysis, [3]Department of Epigenetics, Nagahama Institute of Bioscience and Technology, Nagahama, Shiga 526-0829, Japan

[4]Department of Diagnostic Pathology, Kyoto University Hospital, Kyoto 606-8501, Japan

[5]Division of Hematopoiesis, Center for AIDS Research, Kumamoto University, Kumamoto 860-0811, Japan

[6]Graduate School of Bioscience and Biotechnology, [7]Earth-Life Science Institute, Tokyo Institute of Technology, Tokyo 152-8550, Japan

[8]Yakult Central Institute, Tokyo 186-8650, Japan

[9]RIKEN Center for Integrative Medical Sciences (IMS), Kanagawa 230-0045, Japan

[10]Graduate School of Medicine, Chiba University, Chiba 260-8670, Japan

[11]Graduate School of Medical Life Science, Yokohama City University, Kanagawa 230-0045, Japan

[12]PRESTO, Japan Science and Technology Agency, Saitama 332-0012, Japan

[13]Co-first author

[*]Correspondence: rshinkura@bs.naist.jp (r_shinkura@nagahama-i-bio.ac.jp)

ABSTRACT

Immunoglobulin A (IgA) is the main antibody isotype secreted into the intestinal lumen. IgA plays a critical role in the defense against pathogens and in the maintenance of intestinal homeostasis. However, how secreted IgA regulates gut microbiota is not completely understood. In this study, we isolated monoclonal IgA antibodies from small intestine of healthy mouse. As a candidate of efficient gut microbiota modulator, we selected a W27 IgA that binds to multiple bacteria but not beneficial ones such as *Lactobacillus casei*. W27 could suppress the cell growth of *Escherichia coli* but not *Lactobacillus casei in vitro*, indicating an ability to improve the intestinal environment. Indeed W27 oral treatment could modulate gut microbiota composition and have therapeutic effect on both lymphoproliferative disease and colitis models in mice. Thus W27 IgA oral treatment is a potential remedy for inflammatory bowel disease, acting through restoration of the host-microbial symbiosis.

Dysbiosis of gut microbiota disrupts intestinal homeostasis and causes inflammatory bowel disease (IBD), such as Crohn's disease and ulcerative colitis (UC). Hence restoration of gut microbiota symbiosis is a key to prevention and treatment of IBD [1-3]. One of the promising agents shown to shape the gut microbiota community is intestinal IgA [4-7]. Intestinal IgA is thought to comprise two types; one is high-affinity IgA that is produced by somatic hypermutation (SHM) process in germinal center (GC) B cells and reacts specifically to pathogens and their toxins in a Fab-dependent manner, and the other is poly-reactive IgA that is produced by GC-independent process and recognizes a variety of commensal bacteria probably in a Fab-independent manner [4,5,8]. IgA coating of commensal bacteria was originally discovered as early as in 1968[9]. A recent study refocused IgA coating and suggested that intestinal IgA selectively coated disease-associated commensal bacterial taxa [7, 10], although how IgA can specifically select colitogenic bacteria remained unclear.

Our previous studies revealed that even in the absence of pathogens mice that lack whole IgA (activation-induced cytidine deaminase (AID) deficient mice) and mice that lack only high-affinity IgA due to SHM defect (AID^{G23S} (glycine to serine at the

86 23rd amino acid) mutant mice) developed immune hyperactivation and
87 dysbiosis-associated lymphoproliferative disease [11,12]. These data demonstrate that only
88 high-affinity IgA, but not low-affinity IgA, plays a crucial role in the control of
89 commensal gut microbiota as well as of pathogens. Since gut microbiota contain a huge
90 number of variable species, we thought that only poly-reactive IgA could shape and
91 maintain microbial community in a steady state. Therefore we hypothesized that
92 high-affinity poly-reactive IgA could be a useful gut commensal modulator to restore
93 symbiosis.

94

95 In this study, we isolated monoclonal IgA antibodies and identified their target
96 bacterial epitopes. Interestingly more than 90% of monoclonal IgAs derived from small
97 intestine of mice recognized an epitope, which represented four amino acids (EEHI)
98 expressed in a bacterial enzyme, serine hydroxymethyltransferase (SHMT). Among
99 those IgAs, we selected a high-affinity poly-reactive W27 IgA as the best candidate for
100 an efficient gut microbiota modulator and showed that W27 oral treatment modulated
101 gut microbiota composition and had therapeutic effect on both lymphoproliferative
102 disease and colitis models in mice.

RESULTS

Establishment of IgA Monoclonal Antibodies and Selection of High-affinity Poly-reactive IgA, W27

We thought that the best commensal microbial modulator, which is high-affinity poly-reactive IgA, must be produced through intact SHM process in wild type mice. Therefore we generated hybridomas from intestinal lamina propria (LP)-derived IgA-secreting cells of unimmunized wild type (C57BL/6) mice kept under specific pathogen free (SPF) condition. We isolated 16 monoclonal IgAs, each carrying unrelated sequence of variable region gene in the immunoglobulin heavy chain (V_H) (**Supplementary Table 1**). We tested their binding ability against 14 different cultivable commensal bacterial strains with an ELISA assay. All of the 16 monoclonal IgAs recognized at least three different bacterial strains at antibody concentration of 1.4 μg/ml (**Fig. 1a**).

We selected four clones (W2, W27, W34, W43) producing antibodies in relatively high amounts, and tested their relative binding ability against 14 different strains with a dose-dependent ELISA assay. Among four IgAs, W27 had the most potent reactivity against 12 out of the 14 bacterial strains (**Fig. 1b** and **Supplementary Fig. 1**). Interestingly, W27 bound to each bacterial strain with variable binding strength. The relative reactivities of W27 to *Escherichia coli, Staphylococcus lentus,* and *Pseudomonas fulva* were about 100 times higher than that of W2, while those of W27 to *Bifidobacterium bifidum* and *Blautia coccoides* (previously classified as *Clostridium (C.) coccoides,* one of beneficial bacteria which induces $FoxP3^+$ regulatory T cells) [13] were only 10 times higher than that of W2. W27 had very weak reactivity, if any, to *Lactobacillus casei* (a species of genus *Lactobacillus* generally considered to be probiotic) (**Fig. 1b**). We assume that W27 is the best candidate for commensal microbiota regulator, because it selectively binds to a series of commensal bacteria (including potentially colitogenic one) rather than beneficial ones such as *Bifidobacteirum bifidum, Blautia coccoides* and *Lactobacillus casei*.

High-throughput Analysis of W27-binding bacteria

We further analyzed W27 selective binding ability by IgA-seq of sorted

W27-binding and W27-non-binding gut bacteria from gut contents of IgA-null AID$^{-/-}$ mice (**Fig. 1c**). Family level analysis identified *Porphyromonadaceae*, *Prevotellaceae* and *Lactobacillaceae* as W27-binding bacteria and *Lachnospiraceae* and *Ruminococcaceae* as W27-non-binding bacteria (**Fig. 1c**). A previous study[7] demonstrated that high IgA-coating identified colitogenic bacteria in a mouse colitis model as well as in IBD patients. In their study[7] and in other report[14], *Lactobacillaceae* and *Prevotellaceae* appeared as potentially colitogenic commensal bacteria, whereas *Lachnospiraceae* and *Ruminococcaceae* were recognized as beneficial bacteria *e.g.*, as Tregs inducers[13, 15]. These findings suggested that W27 could change gut microbiota to symbiotic balance, through selective binding to colitogenic bacteria rather than beneficial bacteria.

Mouse Intestinal IgAs Recognize an *E. coli* Enzyme SHMT

We further tried to identify the target molecule of IgA clones through Western blot analysis with comparable amounts of cell lysate from seven different bacterial strains, including a commercially available *E. coli* strain (DH5α), a mouse cell line (NS-1) and a human cell line (293T). Four IgA monoclonal antibodies (W27, W2, W34, W43) revealed visible target bands for DH5α, *E. coli* (a strain isolated from mouse

155 faeces), and *Pseudomonas fulva*. In contrast, all four IgAs did not recognize any protein
156 in *Staphylococcus lentus, Lactobacillus casei, Blautia coccoides, Bifidobacterium*
157 *bifidum*, NS-1 and 293T cells, except for ambiguous bands for *Blautia coccoides* on
158 W27 blot (**Fig. 2a** and **Supplementary Fig. 6**). This suggests that the specific target
159 protein of four IgAs is most likely a common molecule expressed by *E. coli* and
160 *Pseudomonas fulva* (**Fig. 2a** and **Supplementary Fig. 6**). We performed mass
161 spectrometry analysis of a target protein from DH5α cell lysate and found that the target
162 molecule of W27 was an enzyme serine hydroxymethyltransferase (SHMT).
163 Interestingly, the other independent IgA clones (W2, W34 and W43) also recognized
164 Myc-tagged cloned *E. coli* SHMT as well as endogenous SHMT (**Fig. 2b** and
165 **Supplementary Fig. 6**). SHMT is an important metabolic enzyme that catalyzes the
166 reversible methylation reaction of serine and tetrahydrofolate (THF) to glycine and
167 5,10-methylene THF. In the previous studies, SHMT was detected in the periplasm
168 fraction of *E. coli* [16-18], suggesting that IgA could recognize SHMT on the surface of *E.*
169 *coli*.
170
171 **Epitope of SHMT recognized by W27**
172 According to our database search, the gene encoding SHMT, *glyA*, is not found

in the genome of *Bifidobacterium bifidum*, but a wide range of bacteria have the gene. To check whether W27 also recognizes the SHMT proteins in other bacterial species, we cloned the full-length *glyA* gene encoding SHMT from *Pseudomonas fulva*, *Staphylococcus lentus, Lactobacillus casei, Blautia coccoides* as well as the human SHMT. Then we overexpressed their Myc-tagged SHMT proteins in 293T cells. As shown in **Fig. 2c** and **Supplementary Fig. 6**, W27 recognized SHMT of *Pseudomonas fulva* as well as of *E. coli*, but not other bacterial or human SHMT proteins. It suggests that W27 can distinguish the differences in amino acid sequences of each distinct bacterial SHMT.

Indeed further epitope mapping study of *E. coli* SHMT revealed that W27 specifically recognized the peptide SHMT-P1 (AA25-AA45 of *E. coli* SHMT) (**Fig. 2d** and **Supplementary Fig. 6**). Through alignment of amino acid sequences of SHMT from different species, we found the highly conserved motif (RQ-XXXX-ELIASEN) in the N-terminal region of SHMT and further identified four amino acids (EEHI) in the middle of conserved motif (RQ-XXXX-ELIASEN) as a critical determinant of the W27 binding, which is shared by *E. coli* and *Pseudomonas fulva* (**Fig. 2d** and **Supplementary Fig. 6**). To ensure that the residues EEHI were the core epitope

sequence, we generated and overexpressed mutant *E. coli* SHMT protein (replacing EEHI with EHNI) and mutant *Lactobacillus casei* SHMT replaced reciprocally in 293T cells. Western blot analysis clearly showed that W27 specifically recognized EEHI but not EHNI in SHMT (**Fig. 2e** and **Supplementary Fig. 6**), indicating that EEHI is a critical target sequence for W27.

We further confirmed that W27 had the most potent reactivity to SHMT-P1 among the four IgA clones with dose-dependent binding assay (**Fig. 2f**). Interestingly, the other IgA antibodies (W2, W34 and W43) also recognized the same SHMT-P1, whereas myeloma-derived mouse IgA (mIgA) did not recognize it at all (**Fig. 2f**), suggesting that SHMT-P1 is a common bacterial target for intestinal IgA. Indeed forty-two out of forty-four monoclonal IgAs, including sixteen clones shown in **Fig. 1a** and additional monoclonal IgAs derived from other mice, could bind to the peptide containing EEHI sequence (**Supplementary Fig. 2**). According to our database search, *E. coli* shares EEHI amino acid sequence not only with *Pseudomonas fulva* (**Fig. 2d**) but also with variable pathogenic bacteria, including *Haemophilus influenzae*, *Klebsiella pneumoniae, Legionella pneumophila, Salmonella paratyphi A, Salmonella typhimurium* and *Shigella flexneri*, etc. (**Supplementary Table 2**). It is reasonable that

most of intestinal IgAs recognize the EEHI sequence in view of mucosal defense.

Bacterial Growth Suppression by W27 IgA

Our hypothesis agrees with the idea that IgA-binding of colitogenic bacteria may improve dysbiosis [5,7]. However, its mechanism is unknown. One possibility is that high-affinity IgA such as W27 may inhibit bacterial cell growth by binding, but do not affect the cell growth of non-binding beneficial bacteria, leading to the establishment of host-microbiota symbiosis. To prove this hypothesis, we tested if W27 binding could have any effect on bacterial cell growth. For *in vitro* growth assay, we purified W27 by affinity chromatography against SHMT-P1 peptide. The purified fraction of W27 mainly consisted of oligomers (**Supplementary Fig. 3**). Co-culture of affinity-purified W27 and DH5α cells significantly inhibited their cell growth in a dose-dependent manner (**Fig. 3a**), whereas non-binding mIgA (derived from myeloma cells, **Fig. 3b**) did not affect it at all (**Fig. 3a**). By contrast, the cell growth of *Lactobacillus casei* that were not bound by W27 (**Fig. 1b, Fig. 3b**) was not altered by W27. These suggest that binding of bacteria by W27 can suppress their cell growth.

It has been demonstrated that IgA bound to bacteria via Fab-independent,

non-specific manner [4-6,8, 9]. We took advantage of SHMT-deficient *E. coli* (JW2535) (**Fig. 3e** and **Supplementary Fig. 6**) [19]. Since SHMT is one of the key enzymes for the one-carbon metabolism, JW2535 cells exhibits growth retardation as reported previously (**Fig. 3c**) [20]. W27 suppressed only wild type (ME9062) cell growth significantly and did not affect SHMT-deficient cell (JW2535) growth (**Fig. 3c**), although W27 bound to both strains equally (**Fig. 3d, f**). Our results indicated that W27 had an inhibitory effect on *E. coli* cell growth via SHMT-recognition.

Oral Treatment of W27 Improved Lymphoproliferative Disease and Associated Pathological Crypt Damage in AID^{G23S} Mice

We reasoned that the proposed role of W27 to modulate intestinal microbiota leading to symbiosis had to be confirmed in an *in vivo* model lacking high affinity IgA antibodies. Currently, AID^{G23S} knock-in mice are the best candidate mice [12]. We examined whether oral supplementation of W27 could prevent lymphoproliferation in AID^{G23S} mice. W27 (partially purified through ammonium sulfate precipitation, **Supplementary Fig. 3**) was given to AID^{G23S} mice in the drinking water at concentration of 25 μg/ml for four weeks. As a control treatment, low-affinity, poly-reactive IgA (W2, see **Fig. 1b** and **2f**) was given to AID^{G23S} mice in the same

manner. These IgA antibodies consisted of both monomer and oligomer forms and were stable in the drinking water for at least seven days (**Supplementary Fig. 3**). They were delivered through the whole intestine and could be recovered from faeces (**Supplementary Fig. 4**).

Compared to those of untreated AID^{G23S} mice suffering from GC B cell hyperplasia, GC B cell numbers in Peyer's patches (PPs) of W27-treated AID^{G23S} mice were significantly decreased ($p < 0.01$), down to the level of those of wild-type mice (**Fig. 4a**). On the other hand, W2 treatment did not affect it significantly (**Fig. 4a**). Furthermore 30 μg of W27 (affinity-purified) was given by gavage twice a week to IgA-null $AID^{-/-}$ mice suffering more prominent GC hyperplasia than AID^{G23S} mice. Oral W27 treatment for four weeks significantly decreased GC B cell numbers in PPs of $AID^{-/-}$ mice (**Fig. 4b**). In addition, diffuse crypt atrophic damage found in eight (> 30% of total colonic length) and two (5-30% of total colonic length) out of thirty AID^{G23S} mice at 12-16 weeks of age was not observed in any of the thirteen W27-treated AID^{G23S} mice (**Fig. 4c, d**). We concluded that W27 oral supplementation could prevent lymphoproliferative disease and associated crypt damage in AID^{G23S} and $AID^{-/-}$ mice.

Oral W27 Treatment Changed Gut Microbiota Composition

We questioned whether W27 IgA directly affected gut microbiota composition. Through bacterial 16S rRNA meta sequencing, we found that W27 oral administration to AID^{G23S} mice induced a significant change in the relative abundance of 12 different bacterial families (**Fig. 4e**). The relative abundance of *Lachnospiraceae* and *Ruminococcaceae* were significantly increased after W27 oral treatment (**Fig. 4e)**. These bacterial species are generally considered as beneficial Tregs inducers[13, 15]. On the other hand, *Prevotella* and *Lactobacillaceae,* plausible colitogenic bacteria[7, 14], decreased in relative abundance in response to W27 treatment (**Fig. 4e**). In good agreement with our W27 IgA-seq data (**Fig. 1c**), bacteria bound strongly by W27 such as *Lactobacillaceae* and *Prevotellaceae* were decreased in faeces after W27 oral treatment, while bacteria bound weakly by W27 such as *Lachnospiraceae* and *Ruminococcaceae* were increased in faeces after W27 oral treatment (**Fig. 1c** and **4e**). In addition, our quantitative PCR analysis[21] revealed that W27 oral treatment significantly increased the absolute numbers of *Blautia coccoides* group (corresponding to *Lachnospiraceae* in 16S rRNA analysis) and *Clostridium leptum* group (corresponding to *Ruminococcaceae* in 16S rRNA analysis) (**Supplementary Fig. 5,** left half **and**

Supplementary Table 3), whereas W2 (low-affinity IgA) oral treatment did not change them except for a slight decrease of *Prevotella* (**Supplementary Fig. 5**, right half). The significant shift in composition of the microbiota after W27 oral treatment was further confirmed at individual mouse level ($p < 0.05$) (**Fig. 4f**). Thus, as expected from its beneficial effect on lymphoproliferative disease, W27 oral treatment modulated gut microbiota composition towards symbiosis.

W27 Oral Treatment Showed Beneficial Effect on the Experimental Colitis in Mice by Modulating Gut Microbiota

We addressed the question whether W27 oral treatment could prevent colitis induced by dextran sodium sulfate (DSS). As shown previously, when dysbiosis was induced in wild type mice by cohousing them with colitogenic mice or by exposing them to colitogenic bacteria, those mice showed more severe body weight loss than untreated wild-type mice in DSS-induced colitis experiment[7]. Since W27 targets dysbiosis, but not inflammation itself, we assume that W27 supplementation may improve the severity of DSS-induced colitis in mice suffering from dysbiosis. To induce dysbiosis in wild type mice, we gave repeatedly DSS in the drinking water with intervals with the supplementation of W27 in the drinking water or water only (**Fig. 5a**).

298 W27 oral treatment significantly reduced the body weight loss and the increase in
299 disease activity index [22] (**Fig. 5a, b**). A previous study [7] showed that IgA-binding
300 proportion of intestinal bacteria was significantly increased in IBD patients and in a
301 mouse model of colitis. At the end of the experiment, in W27-treated mice, IgA-binding
302 proportion of faecal bacteria was significantly decreased compared to that in control
303 mice (**Fig. 5c**), suggesting the improvement of gut microbial composition by W27.
304 Indeed 16S rRNA analysis revealed the significant difference of microbial composition
305 between W27-treated and untreated mice **(Fig. 5d)**.
306
307 Finally, we tested whether W27 could prevent another colitis model induced by
308 adoptive transfer of $CD4^{+}CD45RB^{high}$ T cells in $Rag1^{-/-}$ mice in an independent other
309 animal facility. W27 treatment clearly ameliorated wasting disease (**Fig. 5e**) associated
310 with chronic colitis[23] (**Fig. 5f, g**). We confirmed that microbiota composition between
311 W27-treated and untreated mice was significantly different at three weeks after T cell
312 transfer (**Fig. 5h**). Since microbial condition in each animal facility was not identical,
313 additional studies are required to define the dysbiosis condition that W27 can target.
314 However, our data suggest that W27 oral treatment can have beneficial effect on colitis
315 that originates through different mechanisms but is associated with dysbiosis.

316

DISCUSSION

In this study we isolated a monoclonal IgA antibody W27 that had strong binding ability against a variety of bacteria and suppressed the cell growth of *E. coli* via an epitope-specific binding, but neither bind to nor suppress *Lactobacillus casei in vitro*. In gut lumen, orally given W27 modulated commensal microbiota composition towards symbiotic balance, resulting in beneficial effects on several dysbiosis-associated disease models in mice.

Recent studies showed that secreted intestinal IgA could recognize and bind to a subset of commensal bacteria that preferentially affect IBD susceptibility in mice and human patients[7, 10]. Such subset of bacteria may vary depending on environment such as mouse facilities and it is difficult to identify a disease-causing bacterium in each human patient. A new approach based on targeted microbial modulation such as W27 oral treatment may overcome this difficulty and contribute to the cure of IBD patients, since W27 selectively binds preferably to multiple colitogenic bacteria through its epitope-specific recognition. However, several questions of critical importance have never been solved.

We demonstrated that simple IgA coating of bacteria did not always inhibit the bacterial growth. Our finding agreed with an early paper published in 1968 demonstrating that certain bacteria continued to grow despite being IgA-coated [9]. Thereafter non-specific binding has been thought to occur via carbohydrates on bacterial cell surface and IgA molecule [8]. Recently Mathias *et al*. has demonstrated the significant difference in IgA binding on cell surface between *E. coli* strains and *Lactobacillus*[24]. Their results showed that the interaction of the three tested Gram-negative bacteria (*E. coli* strains) with deglycosylated or native IgA proteins resulted in similar high level binding, while the interaction of Gram-positive bacteria such as *Lactobacillus* and *Bifidobacterium* was lost by deglycosylated IgA, suggesting a selective role of carbohydrates in the binding of Gram-positive bacteria. In good agreement with these findings, we observed equal levels of surface binding of W27 to *E. coli* strains, ME9062 and JW2535 (**Fig. 3d, f**), indicating the epitope (SHMT)-independent binding on *E. coli* by W27 IgA. A future study is required to determine the unknown molecular patterns involved in IgA binding to *E. coli*.

We addressed a question what type of molecule W27 IgA recognizes to control the diversified commensal bacteria. We identified the epitope of W27 at the amino acid

353 residue level. W27 recognized EEHI sequence of SHMT in highly specific manner (**Fig.**
354 **2d, e**). To understand the physiological importance of EEHI motif in SHMT, we
355 searched the bacterial species that share EEHI in SHMT among 2739 strains whose
356 genome sequences were available. They were mostly *Gammaproteobacteria* and
357 *Betaproteobacteria* species, including a lot of pathogens (**Supplementary Table 2**).
358 Since we generated IgA-producing hybridomas from unimmunized mice kept under
359 SPF condition, the mice had never been exposed by those pathogens listed in
360 **Supplementary Table 2**. The intestinal IgA that reacted with the EEHI sequence,
361 however, seemed to be preferentially selected *in vivo* (**Supplementary Fig. 2**). On the
362 other hand, from our database search, we found that the bacterial species that do not
363 have a *glyA* gene encoding SHMT included several beneficial probiotic bacteria such as
364 *Bifidobacterium bifidum BGN4* and *Faecalibacterium prausnitzii L2-6*, etc. Thus, for
365 both the mucosal defense and the maintenance of symbiosis, the EEHI sequence that we
366 identified can be a key sequence of bacterial selection by IgA in mice. It is of worth to
367 identify the corresponding target sequence in humans.
368

METHODS

Animal Experiments

Unless specifically mentioned, mice were kept and bred under SPF conditions at Nagahama Institute of Bioscience and Technology. The Animal Research Committees of Nagahama Institute of Bioscience and Technology, Yakult Central Institute and IMS-RCAI approved all animal experiments. Unless otherwise mentioned, almost equal numbers of males and females of BALB/c background mice were used for all mouse studies. All mice were from 8 to 18 week old of age, except for the mice used in **Fig. 1c**. No statistical methods were used to predetermine sample size. Animals were not randomized and the data collected were not blinded. The investigators were not blinded to allocation during experiments and outcome assessment except for the experiments in **Fig. 5f**.

Hybridoma Generation

Small intestines were collected and opened longitudinally, washed with PBS to remove all luminal contents, and shaken in PBS containing 5 mM EDTA for 20 min at 37°C. Epithelial cells were removed, and lamina propria layers were cut into small pieces and

incubated with RPMI1640 containing 2% fetal bovine serum, 0.5 mg/ml collagenase and 0.5 mg/ml dispase for 1 h at 37°C with shaking. After the remaining tissues were removed, isolated lamina propria cells were washed with PBS and fused with NS-1 cells using PEG. Cell fusion and subcloning method followed the manufacturer's protocol (ClonaCell-HY Hybridoma Cloning Kit, STEMCELL Technologies). IgA-secreting hybridomas were selected by standard sandwich ELISA with goat anti-mouse IgA (Southern Biotech) and alkaline phosphatase-conjugated goat anti-mouse IgA (Southern Biotech).

IgA Preparation for ELISA and oral treatment of mice

The ascites from RAG2$^{-/-}$Jak3$^{-/-}$ mice [25] injected intraperitoneally with IgA-producing hybridoma or culture supernatants of IgA-producing hybridoma were collected and filtered. Equal volume of saturated ammonium sulfate solution was added to precipitate IgA antibodies. After incubation at 4°C for 24 hours, samples were centrifuged for 20 min at 10,000*g* and 4°C. The pellet was reconstituted with 50% ammonium sulfate solution and centrifuged again. Finally the pellet was reconstituted with PBS, followed by buffer change to PBS on PD-10 column (GE Healthcare).

IgA Affinity-Purification for Immunoblot Analysis, Bacterial Growth Inhibition Assay and Flow Cytometry

Antibody solutions precipitated with ammonium sulfate solution as above were further purified by affinity chromatography on HiTrap™ column (GE Healthcare) conjugated with SHMT-P1-BSA for W27 or HiTrap™ column conjugated with goat anti-mouse IgA antibody (Southern Biotech) for W2, W34 and W43. Standard ELISA determined concentration of each purified IgA antibody. For bacterial growth inhibition assay, purified mouse IgA purchased from Immunology Consultants Laboratory, Inc. was applied onto PD-10 column to eliminate sodium azide and incubated with DH5α cells.

ELISA for Binding Assay against Bacteria

All bacteria were cultured at 37°C overnight in appropriate media as shown in **Supplementary Table 4** under anaerobic conditions (80% N_2, 10% H_2, 10% CO_2) in an anaerobic chamber (Coy laboratory Products) or in an aerobic chamber. The cells were centrifuged, washed with PBS, and suspended in 0.05 M Na_2CO_3 buffer for coating the plates (NUNC Maxisorp) at the concentration of ~10^8 cells /well, except for *Blautia coccoides* and *Bifidobacterium bifidum* (~10^7 cells /well). Relative binding ability of IgA was detected with alkaline phosphatase-conjugated goat anti-mouse IgA (Southern

Biotech). ELISA plates were incubated at 4°C overnight. Then OD values were estimated.

ELISA for Binding Assay against Synthesized Peptides

Synthesized peptides (SHMT-P1~P3) conjugated with BSA were obtained from Sigma. They were suspended in 0.05 M Na_2CO_3 buffer at 1 μg/ ml for coating the plates. Relative binding ability of purified monoclonal IgA antibodies were measured as described above. OD values were estimated after incubation at 25°C for 30 min.

Immunoblot analysis for bacteria and mammalian cells

All bacteria were cultured under appropriate conditions as described above. NS-1 and 293T cells were cultured in RPMI1640 and DMEM medium respectively supplemented with 10% fetal calf serum, 2-ME and gentamycin. The bacterial cells were centrifuged and suspended in PBS containing 1% NP-40 and a proteinase-inhibitor cocktail (Nacalai). For *Staphylococcus lentus, Lactobacillus casei, Blautia coccoides* and *Bifidobacterium bifidum*, lysozyme (0.2 mg/ml) (WAKO) was added in PBS, then sonicated and incubated for 30 min on ice. Total lysates were denatured for SDS-PAGE. Mammalian cells were centrifuged, washed with PBS and suspended directly in

SDS-buffer for heat denaturation. After electrophoresis, all proteins were transferred on a nitrocellulose filter. The filter was incubated with blocking buffer (LI-COR) followed by 2 μg/ml each purified monoclonal IgA. To detect the bound IgA, goat anti-mouse IgA (Southern Biotech) and IR800-conjugated anti-goat IgG (LI-COR) were used. Then the signals were visualized on Odyssey scanner (LI-COR). To assess the amount of loaded bacterial protein, the duplicated SDS-PAGE gel was stained with Coomassie brilliant blue (Nacalai). For Myc-tagged protein detection, anti-Myc-tag antibody (MBL, clone PL14) and IRDye^{TM}800-conjugated anti-rabbit IgG (Rockland) were used.

Bacterial Cell Growth Inhibition Assay

DH5α and *Lactobacillus casei* were cultured in Brain Heart Infusion Broth (Fluka Analytical) and Difco^{TM} Lactobacilli MRS broth (BD) at 37°C overnight, respectively. Then they were centrifuged, washed with PBS twice and diluted to approximately 300-500 cells/ 25 μl in PBS supplemented with 1% (w/v) BSA and 20% normal rat serum and incubated for three hours at 37°C with or without purified W27 IgA or mIgA (myeloma-derived mouse IgA purchased from Immunology Consultants Laboratory, Inc.). After three hours incubation, DH5α and *Lactobacillus casei* were followed by an additional seven and forty-five hours incubation at 37°C in each growth media for

459 growth suppression assay in **Fig. 3a**. In **Fig. 3c**, ME9062 and JW2535 cells were
460 cultured in LB broth at 37°C overnight. Then they were centrifuged, washed with PBS
461 twice and diluted to approximately 0.8-1.2 x 10^5 cells/ 25 μl in PBS supplemented with
462 1% (w/v) BSA and 20% normal rat serum. The cells were incubated with the designated
463 IgA antibodies at 37°C for three hours and further incubated at 37°C for three hours
464 with LB broth (final concentration, x0.33). Then cells were lysed in buffer A (50 mM
465 Tris-HCl (pH 8.0), 300 mM NaCl, 1 mM EDTA (pH 8.0), 0.5% SDS) on Bead Smash
466 (TOMY), and incubated in the presence of proteinase K (0.2 mg/ml, Nacalai) overnight
467 at 55°C. DNA was isolated by phenol/chloroform extraction and precipitated by ethanol.
468 Finally DNA was dissolved in TE buffer. DNA was then subjected to quantitative PCR
469 with KAPA SYBR® FAST qPCR Kit Optimized for LightCycler® 480
470 (KAPABIOSYSTEMS) with DH5α-specific primers (F:
471 5'-ACCTTCGGGCCTCTTGCC-3' and R: 5'-TTCCTCCCCGCTGAAAGTAC-3') and
472 *Lactobacillus casei*-specific primers (F: 5'-TGGCGCAAGCTATCGCTTTT-3' and R:
473 5'-CGCCGACAACAGTTACTCT-3') to measure cell numbers. DNA samples purified
474 from the corresponding numbers of DH5α and *Lactobacillus casei* cells were used as
475 qPCR standard to obtain the cell number of each sample.
476

Isolation of Bacterial Strains from Mouse Faeces

Fresh faeces from wild-type mice kept in the SPF area of Nagahama Institute were suspended in PBS on Bead Smash (TOMY). Diluted feces with PBS were seeded onto blood-agar plates. The plates were incubated under aerobic or anaerobic conditions at 37°C for two or three days, and individual colonies on the plates were picked up for PCR to identify the 16S rRNA gene sequences. Primers for PCR were as follows: 27F (5'-GGAGRRTTTGATYHTGGYTCAG-3') and 1492R (5'-GGGBTACCTTGTTACGACTT-3'). The resulting sequences were compared with sequences in RDP database and genome database using BLAST to determine close species/strains. Identified colonies were cultured independently and stored for subsequent experiments. For IgA binding screening, we used 14 strains of bacteria, which included six isolated strains from mouse faeces and eight clones purchased from ATCC.

Mass Spectrometry Analysis

Immunoprecipitated proteins with W27 antibody from DH5α cell lysate were electrophoresed on two-dimensional SDS-PAGE gel. W27-bound spot was separated and subjected to standard mass spectrometry. Briefly, the sample was loaded onto a

nano-LC equipped with PicoFrit column (New Objective) directly coupled to a nanospray tip of LCMS-IT-TOF system (Shimadzu).

Construction of SHMT Expression Vector

Full length *glyA* gene encoding SHMT of DH5α was amplified with the following primers: SHMT-NotIF (5'-CCGCGGCCGCCCATGTTAAAGCGTGAAA-3') and SHMT-NotIR (5'-AGAGCGGCCGCCTGCGTAAACCGGGTAAC-3'). Underlined sequences represent the recognition sites for NotI. PCR fragment was cloned into pcDNA3.1 (+) (Invitrogen) with 3 X Myc-tag at its 3'-end. Other primers for cloning of different bacterial strains are shown in **Supplementary Table 5**.

The primers used for mutagenesis were as follows: *E. coli* SHMT mutF (5'-CAGGAACACAACATCGAACTGATCGCC-3'), *E. coli* SHMT mutR (5'-GATGTGGTGGTTCTGACGTACTTTTTC-3'), *L. casei* SHMT mutF (5'-CGTCAGGAGGAGCATATCGAACTCATTGCC-3') and *L. casei* SHMT mutR (5'-TTCGATATGCTCCTCCTGACGCTCTTCTTC-3').

Bacterial Flow Cytometry and Sorting of W27 Binding and Non-binding Bacteria

Gut contents of small intestine, cecum and large intestine from four male $AID^{-/-}$ mice

513 (21 week-old of age) were collected and suspended in 50 ml of PBS. Immunostaining
514 and sorting were performed according to a previous report [7] with minor modifications.
515 Briefly, washed bacteria were suspended in 100 μl PBS containing 1% (w/v) BSA and
516 20% rat normal serum (WAKO), incubated for 20 min on ice, and then stained with 100
517 μl buffer containing 250 μg/ml of W27 for 30 min on ice. Samples were washed three
518 times and then stained with PE-conjugated anti-mouse IgA (eBioscience, clone
519 mA-6E1). IgA coating of bacteria was determined by flow cytometry (**Fig. 3**) was done
520 as shown above. For bacterial sorting from gut contents, MACS sorting was done on LS
521 columns with anti-PE MACS beads (Miltenyi Biotec) according to manufacture's
522 methods. After MACS separation, the W27-binding and W27-non-binding fractions
523 were further purified on cell sorter (FACSAria, BD Biosciences).
524
525 **16S rRNA Gene Sequencing and Analysis for W27 Binding and Non-binding**
526 **Bacteria**
527 Bacterial DNA was isolated and purified according to the literature [26] with minor
528 modifications. In brief, bacterial samples were incubated with 15mg/ml lysozyme
529 (Wako) at 37°C for 1h, followed by incubation with purified achromopeptidase (2000
530 units/ml; Wako) at 37°C for 30min. Then, the samples were incubated with 1% sodium

dodecyl sulfate and 1mg/ml proteinase K (Merck) at 55°C for 1h. DNA was purified by phenol/chloroform/isoamyl alcohol extraction and polyethylene glycol precipitation.

The V4 variable region of the 16S rRNA gene was amplified by PCR with dual barcoded primers as described previously [27]. PCR amplicons were purified by AMPure XP magnetic purification beads (Beckman Coulter, Inc.) and quantified using the Quant-iT PicoGreen ds DNA Assay Kit (Life Technologies Japan, Ltd). The pooled amplicons were sequenced on a MiSeq (Illumina, 2 x 250 bp paired-end reads) according to the manufacturer's instructions. The 16S rRNA reads were processed with Mothur following the mothur MiSeq SOP (http://www.mothur.org/wiki/MiSeq_SOP). In brief, the assembled reads were screened to eliminate reads containing ambiguous bases and then aligned to the SILVA 16S rRNA sequence database. UCHIME [28] removed chimeric sequences. The remaining reads were clustered into 97% identity Operational Taxonomic Units (OTUs) and then assigned taxonomy using Ribosomal Database Project database (trainset9_032012.pds). OTUs of less than 0.01% relative abundance were eliminated, and the resulting OTU table was rarefied to 15,000 reads per samples.

Histology and Immunohistochemistry

Freshly isolated colons were snap frozen embedded in OCT compound (Sakura, Japan) in Swiss roll and stored at -80°C. Cryostat sections (6 μm) were fixed in acetone at -20°C for 5 min and stained with hematoxylin and eosin or with Alcian blue (WAKO) and nuclear fast red. For immunohistochemistry, rabbit anti-mouse IgA was purchased from ROCKLAND antibodies & assays and Alexa Fluor 568 goat anti-rabbit IgG was purchased from Life Technologies. Concentration-matched isotype control antibodies were applied to each immunohistochemical staining to ensure the specificity of antibody.

W27 Oral Treatment of Mice

For all oral treatments of W27 except for **Fig.3b**, W27 (precipitated with ammonium sulfate) in the drinking water (tap water) was administered to mice *ad libitum*. Drinking water with or without W27 was renewed once a week. In the experiment of **Fig. 3b**, 30 μg of affinity-purified W27 in PBS was administered to $AID^{-/-}$ mice with a gastric tube twice a week *ad libitum*.

Flow cytometry analysis for germinal center B cells

567 Peyer's patches were excised from the small intestine. Single-cell suspensions were
568 stained with the following antibodies. The following antibodies were obtained from
569 eBioscience: PE-Cy7-labeled anti-mouse/human CD45R (B220) (RA3-6B2),
570 APC-labeled Streptavidin. Biotinylated peanut agglutinin was obtained from VECTOR
571 Laboratories. Dead cells were excluded by propidium iodide. The stained samples were
572 analyzed on BD Accuri™ C6 (BD Bioscience) and Kalusa software (Beckman Coulter).
573

574 **Bacterial Cell Numbers Analysis for W27 Oral Treatment**

575 Bacterial genomic DNA was isolated as described previously[20]. In brief, faecal samples
576 were suspended in extraction buffer (100mM Tris-HCL, 40mM EDTA (pH 9.0) and
577 10% sodium dodecyl sulfate). Then glass beads (diameter, 0.1 mm TOMY) and
578 buffer-saturated phenol were added to the fecal suspension. The suspensions were
579 mixed vigorously on a FastPrep FP 120 instrument (BIO 101, Vista, Calif.). After
580 centrifugation, the supernatants were collected. Then DNA was extracted with
581 phenol/chloroform. Finally, DNA was reconstituted in TE-buffer. Quantitative PCR
582 (qPCR) amplification and detection were performed in 384-well optical plates on an
583 ABI PRISM 7900HT sequence detection system (Applied Biosystems) with
584 group-specific primers for *Blautia coccoides* group, *C. leptum* subgroup, *Atopobium*

585 *cluster*, *Bacteroides fragilis* group, *Prevotella*, *Eubacterium cylinderroides*,
586 *Lactobacillus* and *Enterobacteriaceae* (See **Supplementary Table 3**) [29-31] DNA
587 samples purified from the corresponding number of cells derived from each type-strain
588 of eight bacterial groups were used as qPCR standard to obtain the number of each
589 bacterial group.

590 We confirmed the uniqueness of amplification for the eight group-specific
591 primer pairs by calculating the percentage of matched rRNA gene sequences in each
592 genus from the RDP database (release 11, update 2) (used for the 16S rRNA genes) [32]
593 and the SILVA Large Subunit Ref database (release 117) (used for the 23S rRNA
594 genes) [33] within one mismatch with the RDP ProbeMatch
595 (https://rdp.cme.msu.edu/probematch/search.jsp) and the SILVA TestPrime programs
596 (http://www.arb-silva.de/search/testprime/). The results are shown in **Supplementary**
597 **Table 3**.

598

599 **DNA Extraction for Sequencing of 16S rRNA Genes**

600 Faeces samples were freeze-dried overnight. Freeze-dried feces were broken with 3.0
601 mm Zirconia Beads in Shake Master (Biomedical Science, Tokyo, Japan). Ten
602 milligrams of feces was suspended in 200 µl of 10% SDS/TE (Sodium Dodecyl Sulfate/

603 Tris-EDTA buffer) buffer. Bacterial cells in buffer were broken with 0.1 mm
604 Zirconia/Silica Beads (BioSpec Products, Inc., USA) by vigorous shaking for 5 min at
605 1,500 rpm. The homogenates were centrifuged to isolate DNA for 10 min at 14,000 rpm.
606 The extracted DNA was purified in phenol/chloroform/isoamyl alcohol (25:24:1)
607 solution, precipitated by adding ethanol and 3M sodium acetate, and stored at -20°C.
608
609 **Sequencing of 16S rRNA Genes**
610 The effects of W27 oral treatment for mice gut microbiota were analyzed by two
611 experiments. (i) Comparison of the mean relative abundances of each family of
612 microbiota before and after W27 oral treatment was conducted by the 454 GS JUNIOR
613 sequencer-based 16S rRNA gene sequencing analysis. (ii) Comparison of 97% identity
614 OTU abundances of microbiota between W27 and water oral treatment to wild type and
615 $AID^{-/-}$ mice in DSS-induced colitis was conducted by the Illumina MiSeq
616 sequencer-based 16S rRNA genes amplicon paired-end sequencing analysis. In both
617 experiments, the 338F (5'-ACTCCTACGGGAGGCAGCAGT-3') [34] and 806R
618 (5'-GGACTACCAGGGTATCTAAT-3') [35] primers were used to amplify 16S rRNA
619 genes of gut microbiota. The mixed samples were prepared by pooling approximately
620 equal amounts of PCR amplicon from each sample and subjected to the 454 GS

621 JUNIOR and Illumina MiSeq sequencer.

622 In the 454 GS JUNIOR sequencer-based analysis, we obtained the high-quality
623 reads after removal of the reads that (i) contained ambiguous nucleotides, (ii) contained
624 < 350 or > 650 nt, and (iii) were associated with an average Phred-like quality score of
625 less than 25 as calculated by the 454 GS JUNIOR sequencer. Both the forward and
626 reverse primer sequences were removed by a TagCleaner (version 0.12) search with
627 allowed three mismatches [36]. Sequence clustering of the high-quality 454 reads was
628 conducted by using the UCLUST (version 6.0.307) with identity > 97%, and query and
629 reference coverage > 80% [28]. Chimeric OTUs were detected and removed if the OTUs
630 were assigned to the chimera in both of the following two methods, (i) a UCHIME
631 (version 6.0.307) [28] reference mode search against the reference gold database
632 (http://drive5.com/uchime/gold.fa), and (ii) a UCHIME de novo mode search.
633 Taxonomic assignment of the high-quality 454 reads was performed by a RDP
634 MultiClassifier (version 1.1) search with bootstrap value > 0.5 [37].

635 In the Illumina MiSeq sequencer-based analysis, we discarded the reads that (i)
636 contained ambiguous nucleotides and (ii) were mapped to the PhiX genome sequence
637 by a Bowtie 2 (version 2.1.0) search with default parameters [38]. After that, each forward
638 and reverse read for the paired-end library was merged by a USEARCH (version

6.0.307) with-fastq_truncqual 7 parameter. Both the forward and reverse primer sequences were removed by a TagCleaner search with allowed three mismatches. We obtained the high-quality reads after removal of the reads that (i) contained < 350 or > 650 nt and (ii) were associated with an average Phred-like quality score of less than 25 as calculated by the Illumina MiSeq sequencer. The 97% identity OTU clustering and chimera filtering were performed in the same way for the 454 GS JUNIOR sequencer-based 16S rRNA genes amplicon sequencing analysis. Compositional differences of the 97% identity OTUs among mice with different treatments were visualized by a hierarchical clustering analysis with Bray–Curtis dissimilarity index, and statistically analyzed by a PERMANOVA in the vegan library of the R software.

DSS-induced Colitis

DSS (MP Biomedicals, M.W. 36,000-50,000) at designated concentration in the drinking water (hypochlorous acid water) was administered to mice *ad libitum*. The mice that died before the end of experiments (two water-treated and one W27-treated mice in **Fig. 5a**) were excluded. Disease activity index was scored based on the criteria[21] (**Supplementary Table 6**) in a non-blinded fashion. The experiments were performed at Yakult Central Institute.

Colitis Induced by Adoptive Transfer of $CD4^{+}CD45RB^{high}$ T Cells

Colitis was induced in $Rag1^{-/-}$ mice (C57BL6) by adoptive transfer of $CD4^{+}CD45RB^{high}$ T cells (C57BL6) as described previously [39]. Histological score was determined as shown in **Supplementary Table 7** [23] in a blinded fashion. The experiments were performed at IMS-RCAI.

Statistics

Statistic analyses were performed by designated procedures described in each Figure legend. $P < 0.05$ was considered significant.

ACCESSION NUMBERS

The nucleotide sequences determined in this study were deposited in the DDBJ Sequence Read Archive with the DDBJ BioProject ID PRJDB3207.

672 **REFERENCES**

1. Hooper, L.V., Littman, D.R. & Macpherson, A.J. Interactions between the microbiota and the immune system. *Science* **336**, 1268-1273 (2012).
2. Huttenhower, C., Kostic, A.D. & Xavier, R.J. Inflammatory bowel disease as a model for translating the microbiome. *Immunity* **40**, 843-854 (2014).
3. Round, J.L. & Mazmanian, S.K. The gut microbiota shapes intestinal immune responses during health and disease. *Nat Rev Immunol* **9**, 313-323 (2009).
4. Brandtzaeg, P. Secretory IgA: designed for anti-microbial defense. *Front Immunol* **4**, Article 222 (2013).
5. Macpherson, A.J. & McCoy, K.D. Independence Day for IgA. *Immunity* **43**, 416-418 (2015).
6. Pabst, O. New concepts in the generation and functions of IgA. *Nat Rev Immunol* **12**, 821-832 (2012).
7. Palm, N.W., *et al.* Immunoglobulin A coating identifies colitogenic bacteria in inflammatory bowel disease. *Cell* **158**, 1000-1010 (2014).
8. Mantis, N.J., Rol, N. & Corthesy, B. Secretory IgA's complex roles in immunity and mucosal homeostasis in the gut. *Mucosal Immunol* **4**, 603-611 (2011).
9. Brandtzaeg, P., Fjellanger, I., & Gjeruldsen, S.T. Adsorption of immune A onto oral bacteria in vivo. *J Bacteriology* **96**, 242-249 (1968)
10. Kau, A.L., *et al.* Functional characterization of IgA-targeted bacterial taxa from undernourished Malawian children that produce diet-dependent enteropathy. *Sci Transl Med* **7**, 276ra224 (2015).
11. Fagarasan, S., *et al.* Critical roles of activation-induced cytidine deaminase in the homeostasis of gut flora. *Science* **298**, 1424-1427 (2002).
12. Wei, M., *et al.* Mice carrying a knock-in mutation of Aicda resulting in a defect in somatic hypermutation have impaired gut homeostasis and compromised mucosal defense. *Nat Immunol* **12**, 264-270 (2011).
13. Atarashi, K., *et al.* Treg induction by a rationally selected mixture of Clostridia strains from the human microbiota. *Nature* **500**, 232-236 (2013).
14. Gevers, D., *et al.* The treatment-naive microbiome in new-onset Crohn's disease. *Cell Host Microbe* **15**, 382-392 (2014).
15. Andoh, A., *et al.* Multicenter analysis of fecal microbiota profiles in Japanese patients with Crohn's disease. *J Gastroenterol* **47**, 1298-1307 (2012).
16. Lasserre, J.P., *et al.* A complexomic study of Escherichia coli using two-dimensional blue native/SDS polyacrylamide gel electrophoresis. *Electrophoresis* **27**, 3306-3321 (2006).

17. Link, A.J., Robison, K. & Church, G.M. Comparing the predicted and observed properties of proteins encoded in the genome of Escherichia coli K-12. *Electrophoresis* **18**, 1259-1313 (1997).
18. Weiner, J.H. & Li, L. Proteome of the Escherichia coli envelope and technological challenges in membrane proteome analysis. *Biochim Biophys Acta* **1778**, 1698-1713 (2008).
19. Baba, T., *et al.* Construction of Escherichia coli K-12 in-frame, single-gene knockout mutants: the Keio collection. *Mol Syst Biol* **2**, 2006 0008 (2006).
20. Nichols, R.J., *et al.* Phenotypic landscape of a bacterial cell. *Cell* **144**, 143-156 (2011).
21. Matsuki, T., *et al.* Quantitative PCR with 16S rRNA-Gene-Targeted Species-Specific Primers for Analysis of Human Intestinal Bifidobacteria. *Applied and Environmental Microbiology* **70**, 167-173 (2004).
22. Cooper, H.S., Murthy, S.N., Shah, R.S. & Sedergran, D.J. Clinicopathologic study of dextran sulfate sodium experimental murine colitis. *Lab Invest* **69**, 238-249 (1993).
23. Asseman, C., Mauze, S., Leach, M.W., Coffman, R.L. & Powrie, F. An essential role for interleukin 10 in the function of regulatory T cells that inhibit intestinal inflammation. *J Exp Med* **190**, 995-1004 (1999).
24. Mathias, A., & Corthesy, B. Recognition of gram-positive intestinal bacteria by hybrid- and colostrum-derived secretory immune A is mediated by carbohydrates. *J Biol Chem* **286**, 17239-17247 (2011).
25 Ono, A., *et al.* Comparative study of human hematopoietic cell engraftment into BALB/c and C57BL/6 strain of rag-2/jak3 double-deficient mice. *J Biomed Biotechnol* **2011**, 539748 (2011).
26 Morita, H., *et al.* An improved DNA isolation method for metagenomic analysis of the microbial flora of the human intestine. *Microbes and environments* **22**, 214-222 (2007).
27 Kozich, J.J., Westcott, S.L., Baxter, N.T., Highlander, S.K. & Schloss, P.D. Development of a dual-index sequencing strategy and curation pipeline for analyzing amplicon sequence data on the MiSeq Illumina sequencing platform. *Appl Environ Microbiol* **79**, 5112-5120 (2013).
28 Edgar, R.C., Haas, B.J., Clemente, J.C., Quince, C. & Knight, R. UCHIME improves sensitivity and speed of chimera detection. *Bioinformatics* **27**, 2194-2200 (2011).
29 Matsuda, K., Tsuji, H., Asahara, T., Kado, Y. & Nomoto, K. Sensitive

quantitative detection of commensal bacteria by rRNA-targeted reverse transcription-PCR. *Appl Environ Microbiol* **73**, 32-39 (2007).

30 Matsuki, T., Watanabe, K., Fujimoto, J., Takada, T. & Tanaka, R. Use of 16S rRNA gene-targeted group-specific primers for real-time PCR analysis of predominant bacteria in human feces. *Appl Environ Microbiol* **70**, 7220-7228 (2004).

31 Rinttila, T., Kassinen, A., Malinen, E., Krogius, L. & Palva, A. Development of an extensive set of 16S rDNA-targeted primers for quantification of pathogenic and indigenous bacteria in faecal samples by real-time PCR. *J Appl Microbiol* **97**, 1166-1177 (2004).

32 Cole, J.R., *et al.* Ribosomal Database Project: data and tools for high throughput rRNA analysis. *Nucleic Acids Res* **42**, D633-642 (2014).

33 Quast, C., *et al.* The SILVA ribosomal RNA gene database project: improved data processing and web-based tools. *Nucleic Acids Res* **41**, D590-596 (2013).

34 Walter, J., *et al.* Detection and identification of gastrointestinal Lactobacillus species by using denaturing gradient gel electrophoresis and species-specific PCR primers. *Appl Environ Microbiol* **66**, 297-303 (2000).

35 Osek, J. Development of a multiplex PCR approach for the identification of Shiga toxin-producing Escherichia coli strains and their major virulence factor genes. *Journal of Applied Microbiology* **95**, 1217-1225 (2003).

36 Schmieder, R., Lim, Y.W., Rohwer, F. & Edwards, R. TagCleaner: Identification and removal of tag sequences from genomic and metagenomic datasets. *BMC Bioinformatics* **11**, 341 (2010).

37 Wang, Q., Garrity, G.M., Tiedje, J.M. & Cole, J.R. Naive Bayesian classifier for rapid assignment of rRNA sequences into the new bacterial taxonomy. *Appl Environ Microbiol* **73**, 5261-5267 (2007).

38 Langmead, B. & Salzberg, S.L. Fast gapped-read alignment with Bowtie 2. *Nat Methods* **9**, 357-359 (2012).

39 Furusawa, Y., *et al.* Commensal microbe-derived butyrate induces the differentiation of colonic regulatory T cell. *Nature* **504**, 446-450 (2013).

673

Correspondence and requests for materials should be addressed to

R.S. (rshinkura@bs.naist.jp).

ACKNOWLEDGMENTS

We thank Dr. T. Honjo for providing AID^{G23S} and $AID^{-/-}$ mice, Dr. Niki for providing *E. coli* strains, ME9062 and JW2535, Dr. S. Nomura and Ms. M. Ohta for important technical help and Drs. T. Nakano, K. Asoh and V. Shivarov for critical reading. This work was supported by grants from The Japan Science and Technology Agency, JSPS KAKENHI 15H04732, Yakult Bio-Science Foundation, Naito Memorial Foundation, Senshin Medical Research Foundation and Astellas Foundation for Research on Metabolic Disorders (to R.S.), and also by AMED-CREST, AMED and RIKEN Pioneering Project “Biology of Symbiosis” (to H.O.).

AUTHOR CONTRIBUTIONS

S.Okai, F.U. and R.S. designed experiments, performed experiments, analyzed data and wrote the paper. S.Okai, S.Y., Y.H., T.N. and M.K. performed pathological analyses. S.M., M.N., T.N., and Y.W. provided live anaerobic bacteria and performed bacterial

qPCR analysis. M.H. performed mass spectrometry. S.Okai, R.S., S.M., E.M., H.O. were involved in induced colitis experiments. E.M. and H.O. performed W27 binding bacterial sorting and related bioinformatics analyses. T.K., H.O., K.Y., E.N., H.M., T.Y. and K.K. performed microbiome bioinformatics analyses for antibody-treated mice. S.Okada provided essential materials. S.Okai, F. U., R.S., S.M., H.O., K.K., H.M., E.M. and T.K. were involved in data discussions.

COMPETING FINANCIAL INTERESTS

The authors declare no competing financial interests.

FIGURE LEGENDS

Figure 1 LP-derived Monoclonal W27 Antibody is Identified as a High-affinity Poly-reactive IgA

(a) Reactivity of 16 monoclonal IgA antibodies against 14 different bacterial strains was evaluated by ELISA assay. Each monoclonal IgA at concentration of 1.4 μg/ml was applied to ELISA plates coated with each strain of bacteria. The positive binding was determined by O.D. value > 0.3. Grey squares, positive binding; open squares, no binding. ND: not determined. * Isolated bacteria from mouse faeces. **(b)** The relative binding ability of each IgA clone was analysed by ELISA assay with serially diluted monoclonal IgA antibodies. O.D., optical density. All data are representative of at least three independent biological experiments **(a** and **b). (c)** Representative FACS bacterial sorting results of Pre-sorted, Sorted W27 binding and Sorted W27 non-binding populations from mixed gut contents of four $AID^{-/-}$ mice (21 weeks of age) (left). Mean relative abundance of operational taxonomic units classified at the family level for each population (right). Data were obtained from five technical replicated sorting and sequencing procedures. Source Data are provided online.

Figure 2 W27 IgA Recognizes an Epitope of the Enzyme SHMT to Target a Set of Bacteria Selectively

(a) The reactivity of four IgAs to cell extracts from seven bacteria, a mouse B cell line (NS-1) and a human cell line (293T). SDS-PAGE gels were applied to either Western blot with antibody (W27, W2, W34, and W43) or Coomassie brilliant blue (CBB) staining to confirm that comparable amounts of each protein were loaded. **(b)** Four IgAs recognized a single molecule, SHMT, in DH5α. Overexpressed Myc-tagged *E. coli* SHMT in DH5α was detected as well as endogenous SHMT. Note that total DH5α lysate amount loaded on each gel was not identical. **(c)** Myc-tagged cloned SHMT proteins derived from five bacteria and human were overexpressed in 293T cells to confirm binding by W27. **(d)** Amino acid (AA) sequences of synthesized three peptides (SHMT-P1~P3) are shown. Conserved and variant amino acid sequences were shown in black and red, respectively. Underlined red residues were the core epitope for W27. **(e)** Myc-tagged mutant SHMT proteins (*E. coli* $SHMT^{mut\text{-}EHNI}$ and *Lactobacillus casei (L. casei)* $SHMT^{mut\text{-}EEHI}$) were overexpressed in 293T cells. **(f)** Relative affinity of each purified IgA against SHMT-P1-BSA. mIgA: myeloma-derived mouse IgA. O.D., optical density. Data are representative from two or three independent biological

738 experiments (**a** to **f**). The entire gels and blots are shown in **Supplementary Fig. 6** (**a** to
739 **e**).
740
741 **Figure 3 W27 Suppressed *E. coli* Cell Growth via SHMT-specific Recognition**
742 (**a**) Three to five hundred cells of DH5α and *Lactobacillus* (*L.) casei* were incubated
743 with affinity-purified W27 or control mouse IgA (mIgA) at the designated concentration
744 for three hours at 37°C. After then the DH5α and *L. casei* cells were incubated with
745 growth medium at 37°C for additional seven and forty-five hours respectively, until the
746 cells grew to reach the comparable cell numbers. ** $P < 0.01$, * $P < 0.05$. ANOVA was
747 performed, followed by Bonferroni-Holm post-hoc tests for multiple comparisons. **(b)**
748 IgA surface staining of *E. coli* and *L. casei.* **(c)** *E. coli* cells (0.8-1.2 x 10^5 cells) were
749 incubated with affinity-purified W27 or control mouse IgA (mIgA) at the designated
750 concentration for three hours at 37°C. After then the samples were incubated for
751 additional three hours with growth medium at 37°C. ** $p < 0.001$ vs. without W27.
752 Statistical analysis was performed by two-sided Mann-Whitney test. ME9062:
753 SHMT-proficient *E. coli*, JW2535: SHMT-deficient *E. coli*. Each dot represents mean
754 of three technical replicates (**a** and **c**). Data were collected from 3-9 independent
755 biological experiments (**a** and **c**). All data are expressed as medians ± range in (**a**) and

(**c**). **(d)** IgA surface staining of ME9062 and JW2535. Open histogram: unstained cells in (**b**) and (**d**). **(e)** Western blot analysis confirmed the SHMT deficiency of JW2535. The entire gel and blot are shown in **Supplementary Fig. 6**. **(f)** Reactivity of W27 and mIgA antibodies against two different bacterial strains was evaluated by ELISA assay. Data are representative from three independent biological experiments (**b, d, e** and **f**).

Figure 4 W27 Oral Treatment Prevented Pathological Colonic Phenotype and Modulated Gut Microbial Composition in AID^{G23S} Mice

(a) Total number of GC B cells ($B220^{+}PNA^{high}$) in PPs from mice. Data are from 2-5 independent biological experiments, except for W2 treatment (one experiment). IgA antibodies (W27, W2) were orally administered to AID^{G23S} mice in the drinking water at concentration of 25 μg/ml for 4 weeks. All data are expressed as means $\pm$ SE. ** $P <$ 0.01. ANOVA was performed, followed by Bonferroni-Holm post-hoc tests for multiple comparisons. **(b)** The PP GC B cell numbers by W27 oral treatment by gavage in $AID^{-/-}$ mice. Data are from three independent biological experiments. All data are expressed as medians $\pm$ range. ** $P <$ 0.01. Statistical analysis was performed by two-sided Mann-Whitney test. **(c)** Representative hematoxylin and eosin (HE) staining of colon from control (upper) and W27-treated (lower) AID^{G23S} mice. Scale bars, 500μm. **(d)**

774 The severity of colonic crypt damage was examined on HE-stained colon sections based
775 on the percentage of affected area of the full-length of the colon. **(e)** Mean relative
776 abundance of operational taxonomic units classified at the family level before (left) and
777 after (right) W27 oral treatment in AID^{G23S} mice (n=4). The bacterial family names were
778 listed only when their relative abundance was changed significantly by W27 oral
779 treatment ($p < 0.05$, Fisher's exact test. Corrected for false discovery rate). **(f)**
780 Hierarchical clustering and PERMANOVA comparing before and after W27 treatment.
781 M1-M4 represents the individual mice. $p < 0.05$. Source Data are provided online (**e** and
782 **f**).
783
784 **Figure 5 W27 Oral Treatment Presented Colitis Induced by DSS and Adoptive**
785 **Transfer of Naïve T Cells.**
786 **(a)** Body weight change. DSS (3.5%) and W27 (25 μg/ml) were given to female
787 BALB/c wild-type mice in the drinking water. Timeline of DSS and W27 treatment is
788 shown below the graph. **(b)** Disease activity index scored as reported previously[22]. **(c)**
789 IgA binding population of faecal bacteria from W27-treated or water control mice at the
790 end of the experiment. **(d)** Faecal microbial composition analysis at the end of
791 experiment by hierarchical clustering and PERMANOVA comparing between

W27-treated and -untreated mice. $p < 0.05$. **(e)** Body weight change after $CD4^{+}CD45RB^{high}$ T cell adoptive transfers into male $Rag1^{-/-}$ mice. **(f)** Histological score according to a previous report[23]. **(g)** Representative colonic sections stained with HE and Alcian blue (AB) with nuclear fast red. Scale bars, 200 μm. **(h)** Faecal microbial composition analysis at three weeks post transfer by hierarchical clustering and PERMANOVA comparing between W27-treated and -untreated mice. $p < 0.05$. Data are expressed as means ± SE. (**a** and **e**), and expressed as medians ± range (**b, c,** and **f**). * $p < 0.05$, ** $p < 0.01$. Two-way repeated measured ANOVA followed by Bonferroni post hoc test (**a** and **e**). Statistical analysis was performed by two-sided Mann-Whitney test (**b, c,** and **f**). **(a)-(d)** One experiment performed at Yakult Central Institute. **(e)-(h)** One experiment performed at RIKEN Center for IMS. Source Data are provided online (**d** and **h**).

Figure 1

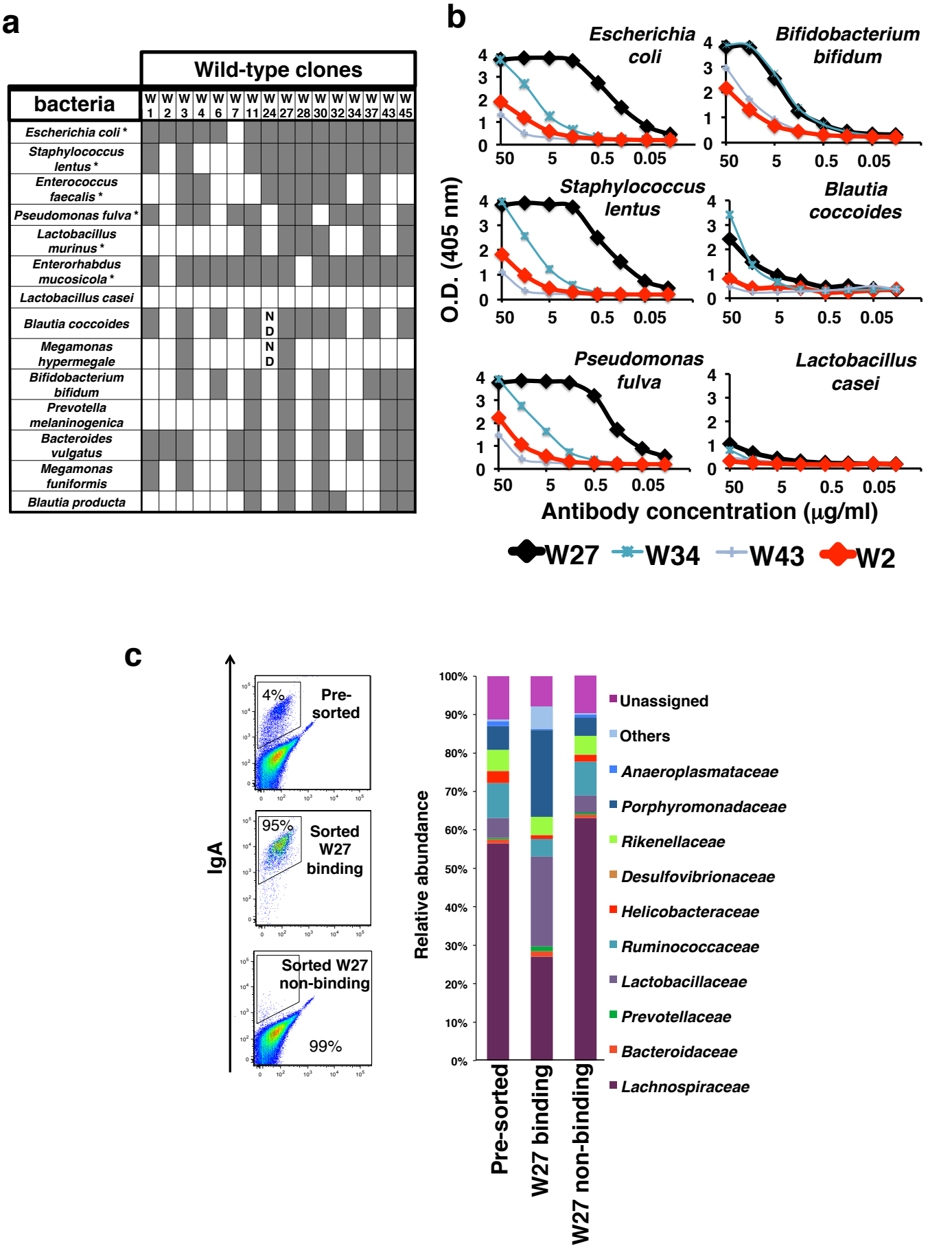
a
Wild-type clones
bacteria
W 1
W 2
W 3
W 4
W 6
W 7
W 11
W 24
W 27
W 28
W 30
W 32
W 34
W 37
W 43
W 45
Escherichia coli *
Staphylococcus lentus *
Enterococcus faecalis *
Pseudomonas fulva *
Lactobacillus murinus *
Enterorhabdus mucosicola *
Lactobacillus casei
Blautia coccoides
Megamonas hypermegale
Bifidobacterium bifidum
Prevotella melaninogenica
Bacteroides vulgatus
Megamonas funiformis
Blautia producta
ND
ND
b
Escherichia coli
Bifidobacterium bifidum
Staphylococcus lentus
Blautia coccoides
Pseudomonas fulva
Lactobacillus casei
O.D. (405 nm)
Antibody concentration (μg/ml)
W27
W34
W43
W2
c
IgA
4%
Pre-sorted
95%
Sorted W27 binding
Sorted W27 non-binding
99%
Relative abundance
Pre-sorted
W27 binding
W27 non-binding
Unassigned
Others
Anaeroplasmataceae
Porphyromonadaceae
Rikenellaceae
Desulfovibrionaceae
Helicobacteraceae
Ruminococcaceae
Lactobacillaceae
Prevotellaceae
Bacteroidaceae
Lachnospiraceae

Figure 2

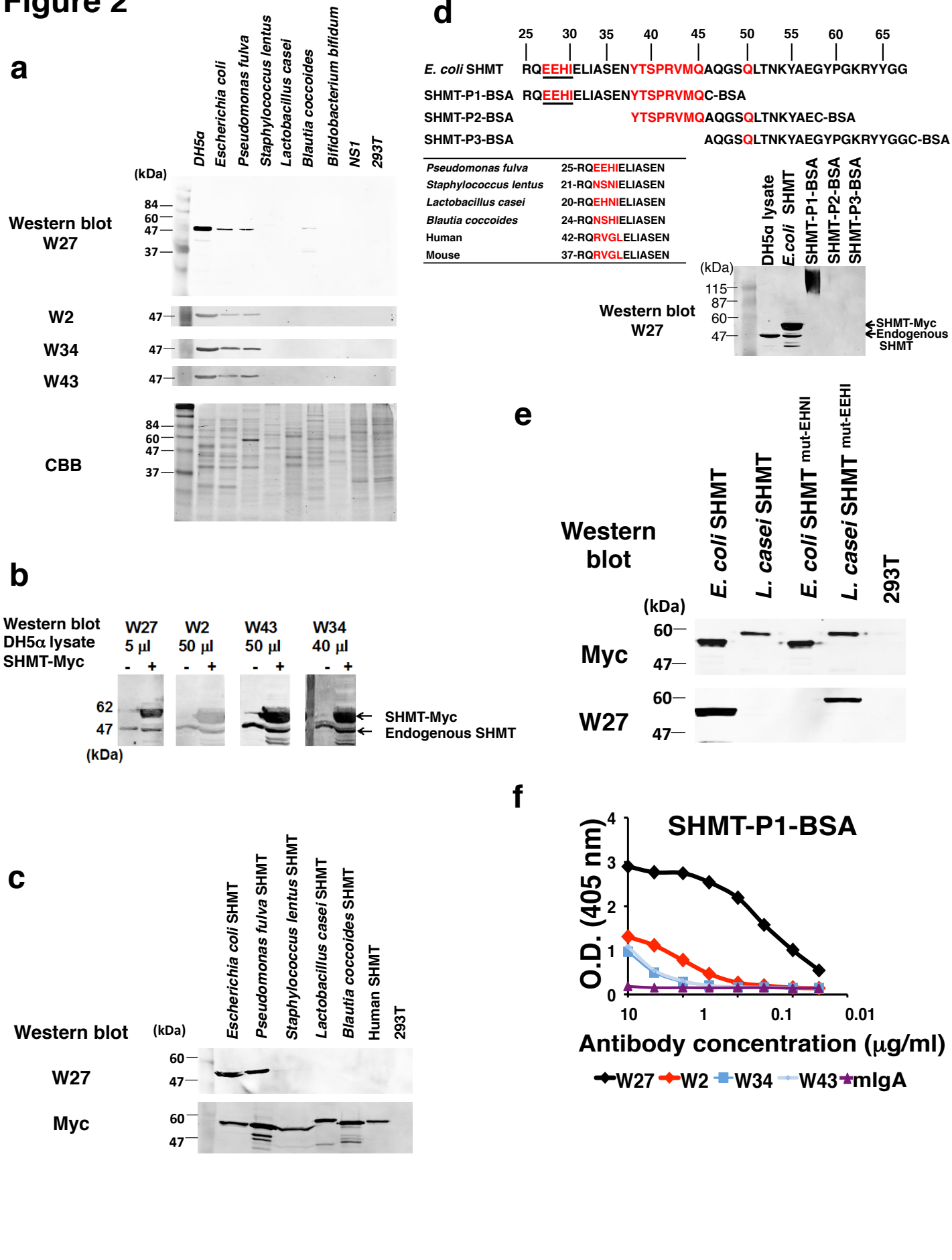
a
DH5α
Escherichia coli
Pseudomonas fulva
Staphylococcus lentus
Lactobacillus casei
Blautia coccoides
Bifidobacterium bifidum
NS1
293T
(kDa)
Western blot
W27
W2
W34
W43
CBB
84
60
47
37
b
Western blot
DH5α lysate
SHMT-Myc
W27
5 µl
W2
50 µl
W43
50 µl
W34
40 µl
62
47
(kDa)
SHMT-Myc
Endogenous SHMT
c
Escherichia coli SHMT
Pseudomonas fulva SHMT
Staphylococcus lentus SHMT
Lactobacillus casei SHMT
Blautia coccoides SHMT
Human SHMT
293T
Western blot
(kDa)
W27
Myc
d
25 30 35 40 45 50 55 60 65
E. coli SHMT RQEEHIELIASENYTSPRVMQAQGSQLTNKYAEGYPGKRYYGG
SHMT-P1-BSA RQEEHIELIASENYTSPRVMQC-BSA
SHMT-P2-BSA YTSPRVMQAQGSQLTNKYAEC-BSA
SHMT-P3-BSA AQGSQLTNKYAEGYPGKRYYGGC-BSA
Pseudomonas fulva 25-RQEEHIELIASEN
Staphylococcus lentus 21-RQNSNIELIASEN
Lactobacillus casei 20-RQEHNIELIASEN
Blautia coccoides 24-RQNSHIELIASEN
Human 42-RQRVGLELIASEN
Mouse 37-RQRVGLELIASEN
DH5α lysate
E.coli SHMT
SHMT-P1-BSA
SHMT-P2-BSA
SHMT-P3-BSA
(kDa)
115
87
60
47
Western blot
W27
SHMT-Myc
Endogenous SHMT
e
Western blot
E. coli SHMT
L. casei SHMT
E. coli SHMT mut-EHNI
L. casei SHMT mut-EEHI
293T
(kDa)
Myc
W27
60
47
f
SHMT-P1-BSA
O.D. (405 nm)
4
3
2
1
0
10
1
0.1
0.01
Antibody concentration (µg/ml)
W27
W2
W34
W43
mIgA

Figure 3

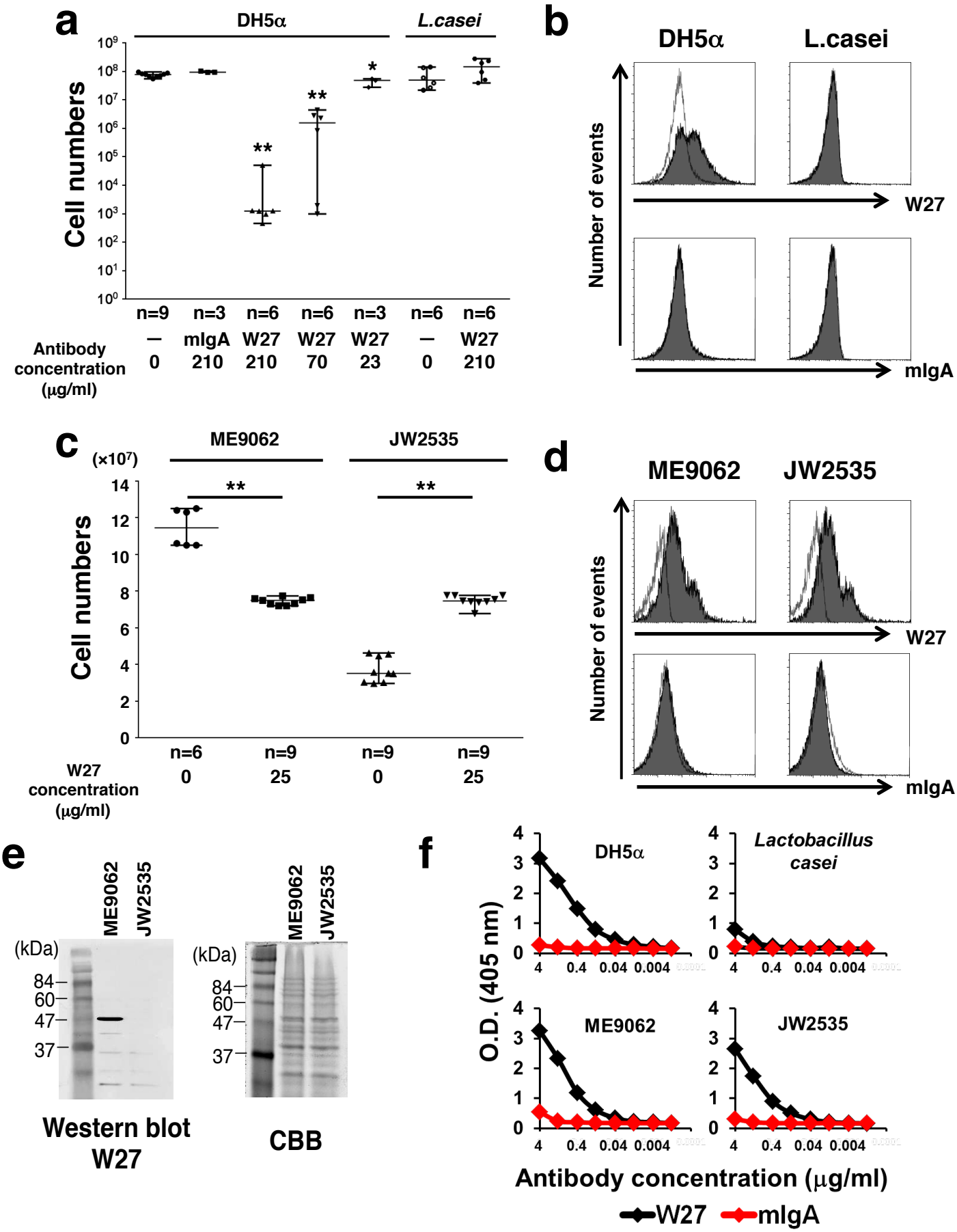
a
DH5α
L.casei
Cell numbers
n=9 n=3 n=6 n=6 n=3 n=6 n=6
Antibody concentration (μg/ml)
— mIgA W27 W27 W27 — W27
0 210 210 70 23 0 210
b
DH5α
L.casei
Number of events
W27
mIgA
c
ME9062
JW2535
(×10⁷)
Cell numbers
n=6 n=9 n=9 n=9
W27 concentration (μg/ml)
0 25 0 25
d
ME9062
JW2535
Number of events
W27
mIgA
e
ME9062
JW2535
(kDa)
84
60
47
37
Western blot W27
CBB
f
DH5α
Lactobacillus casei
ME9062
JW2535
O.D. (405 nm)
Antibody concentration (μg/ml)
W27
mIgA

Figure 4

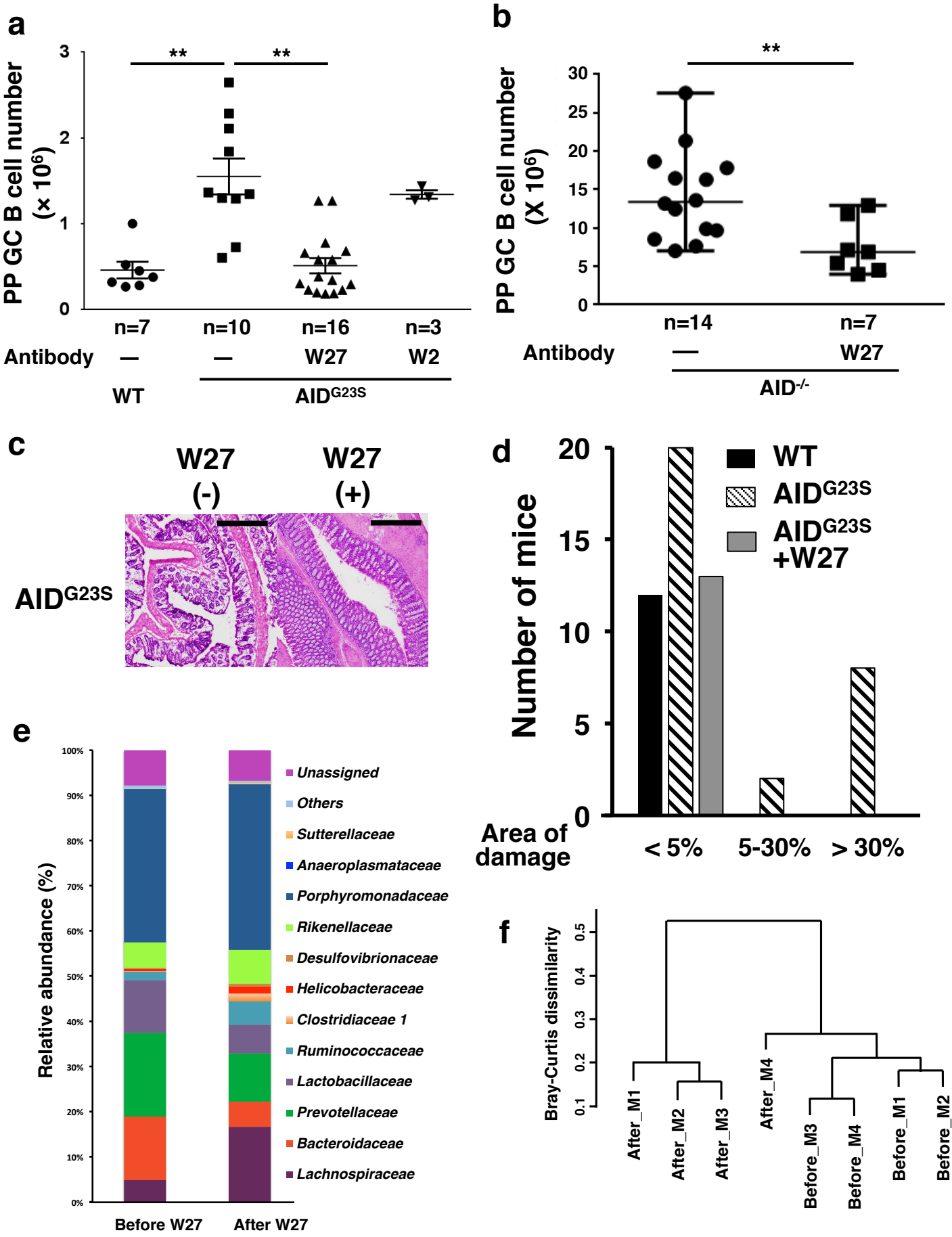
a
PP GC B cell number (× 10⁶)
**
**
n=7
n=10
n=16
n=3
Antibody
—
—
W27
W2
WT
AIDG23S
b
PP GC B cell number (X 10⁶)
**
n=14
n=7
Antibody
—
W27
AID-/-
c
W27 (-)
W27 (+)
AIDG23S
d
Number of mice
WT
AIDG23S
AIDG23S +W27
Area of damage
< 5%
5-30%
> 30%
e
Relative abundance (%)
Unassigned
Others
Sutterellaceae
Anaeroplasmataceae
Porphyromonadaceae
Rikenellaceae
Desulfovibrionaceae
Helicobacteraceae
Clostridiaceae 1
Ruminococcaceae
Lactobacillaceae
Prevotellaceae
Bacteroidaceae
Lachnospiraceae
Before W27
After W27
f
Bray-Curtis dissimilarity
After_M1
After_M2
After_M3
After_M4
Before_M3
Before_M4
Before_M1
Before_M2

Figure 5

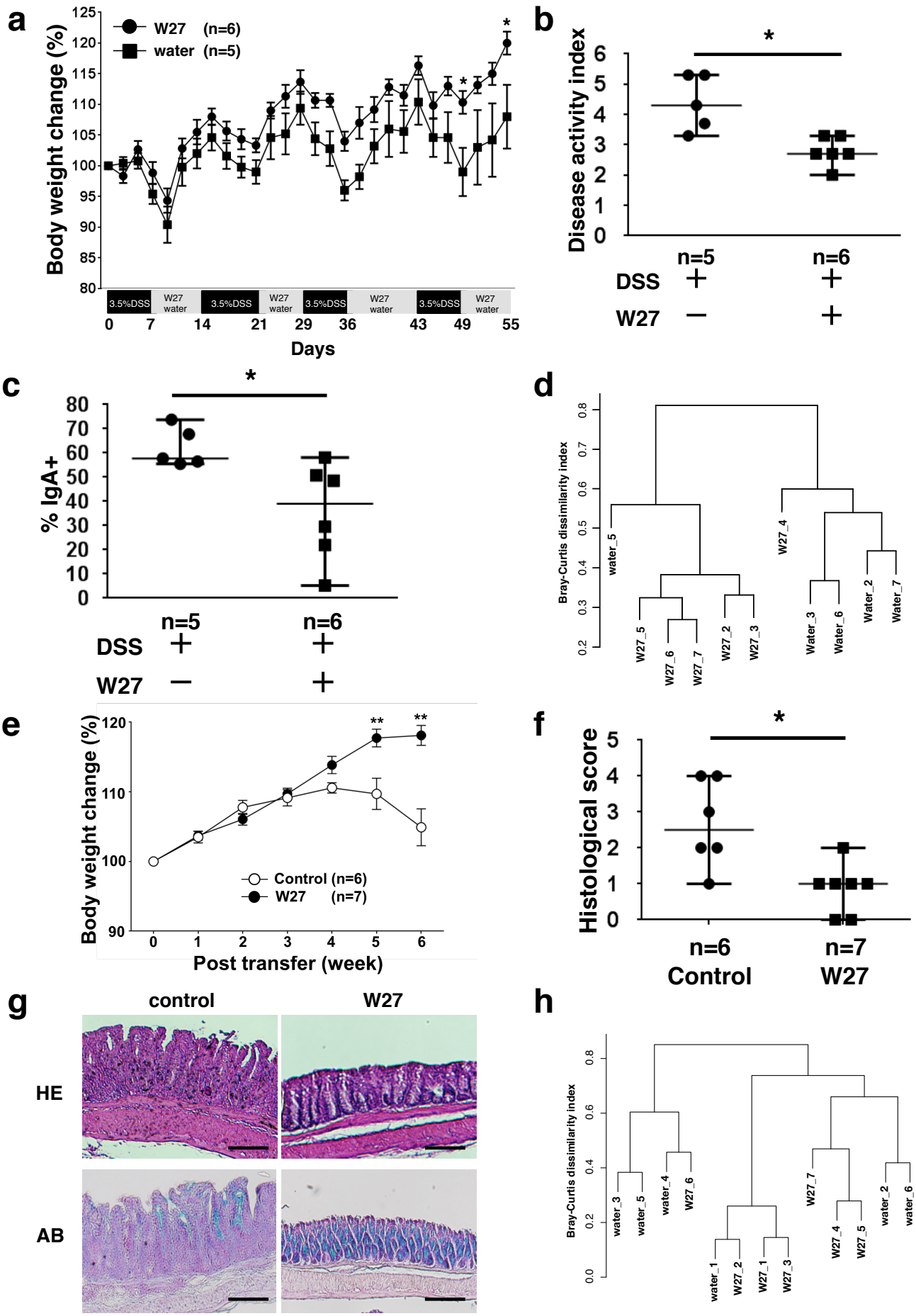
a
W27 (n=6)
water (n=5)
Body weight change (%)
3.5%DSS
W27 water
Days
b
Disease activity index
n=5
n=6
DSS
W27
c
% IgA+
n=5
n=6
DSS
W27
d
Bray-Curtis dissimilarity index
water_5
W27_4
W27_5
W27_6
W27_7
W27_2
W27_3
Water_3
Water_6
Water_2
Water_7
e
Body weight change (%)
Control (n=6)
W27 (n=7)
Post transfer (week)
f
Histological score
n=6
Control
n=7
W27
g
control
W27
HE
AB
h
Bray-Curtis dissimilarity index
water_3
water_5
water_4
W27_6
water_1
W27_2
W27_1
W27_3
W27_7
W27_4
W27_5
water_2
water_6